

# Spinel-type oxide catalysts for low temperature CO oxidation generated by use of an ultrasonic aerosol pyrolysis process

G. Fortunato,<sup>a</sup> H. R. Oswald<sup>a</sup> and A. Reller<sup>b</sup>

<sup>a</sup>*Institute for Inorganic Chemistry, University of Zurich, Winterthurerstr. 190, CH-8057 Zurich, Switzerland*

<sup>b</sup>*Solid State Chemistry, University of Augsburg, Universitätsstrasse 1, 86159 Augsburg, Germany*

Received 8th September 2000, Accepted 4th December 2000

First published as an Advance Article on the web 1st February 2001

The aim of this study was to generate spinel-type oxides by a continuous ultrasonic aerosol pyrolysis procedure and to evaluate the chemical and physical properties of the product powders. The ultrasonic aerosol pyrolysis process consists of three steps, which include “atomisation” of an aqueous metal nitrate solution, transport to the furnace system and controlled thermal decomposition of the precursor aerosol. The synthesis method allows the production of pure  $\text{CuMn}_2\text{O}_4$ ,  $\text{LiMn}_2\text{O}_4$  and  $\text{CuCo}_2\text{O}_4$  spinels, whereas  $\text{NiMn}_{2-x}\text{O}_4$  contains small quantities of  $\alpha\text{-Mn}_2\text{O}_3$ . The powders are finely dispersed, mesoporous products exhibiting a uniform morphology. Scanning electron microscopy reveals that the product is made up of hollow spheres. XRD, TA and XPS results reveal that  $\text{CuMn}_2\text{O}_4$  exists in a metastable state. It segregates in air already at temperatures of 300 °C, whereas in an inert atmosphere the spinel is stable up to 600 °C. XPS measurements indicate the presence of a redox system in the form of  $\text{Cu}^{2+} + \text{Mn}^{3+} \rightleftharpoons \text{Cu}^{1+} + \text{Mn}^{4+}$ , which is one of the main features for the high turnover rates of CO with  $\text{O}_2$  of this catalyst already at room temperature. XPS measurements, after treatment of  $\text{CuMn}_2\text{O}_4$  with CO and  $\text{O}_2$ , confirm the highly reactive surface.  $\text{NiMn}_2\text{O}_4$  and  $\text{CuCo}_2\text{O}_4$  also show high activities in the catalytic CO oxidation.  $\text{LiMn}_2\text{O}_4$  is rather inactive. A comparison of  $\text{CuMn}_2\text{O}_4$  with  $\text{LiMn}_2\text{O}_4$  points to the crucial influence of the copper cations on the conversion rates of the CO oxidation. In the synthesis of  $\text{CuMn}_2\text{O}_4$  the introduction of glucose into the starting metal nitrate solution revealed changed properties of the product powders: as a consequence, the distribution of the cations on the surface is changed and markedly smaller conversion rates for the catalytic CO oxidation are observed.

## Introduction

Research in the field of fine grain, ceramic, mixed oxide systems has gained immense importance due to their potential application in many areas of technology. The conventional ceramic method for the preparation of complex metal oxide systems involves a high calcination temperature and long sintering time, which results in a loss of the fine particle nature. New synthesis strategies circumvent high temperatures and thus offer a promising way to obtain solids with new structural and textural properties. A variety of non-conventional techniques have been used to prepare fine particle systems. This includes, for example, coprecipitation-, sol-gel-, hydrothermal- and aerosol-processes. Aerosol methods have been used to produce a variety of homogenous mixed metal oxides. Analogously, sulfides, nitrides and carbides can be synthesized.<sup>1–3</sup> These studies have shown that this particular method allows the generation of particles with a unique combination of properties that in many cases cannot be achieved by other processes. Their main features are as follows.

(a) Powders are obtained in a single-step, self-contained process. It is possible to form powders and coatings as well as films; even oriented thin films can be produced.<sup>4</sup> The aerosol method provides shadow-free deposition so that it is possible to make coatings even on quartz wool. (b) The method allows an excellent control of chemical homogeneity and stoichiometry.<sup>5,6</sup> (c) The method offers a possibility for the synthesis of multicomponent materials.<sup>3</sup> (d) A suitable choice of the precursor systems results in a control of the morphology of the particles.<sup>7</sup> The extension of spray pyrolysis to systems which include organic additives (fuels) can provide solids with

new properties such as changed morphology,<sup>8</sup> structure, surface composition, *etc.* (e) The settings of the synthesis parameters allow the production of porous or non-porous powders. (f) The particles consist of unagglomerated or soft and hard agglomerates.

The Cu–Mn–O-system is a well known oxidation catalyst for carbon monoxide oxidation with oxygen at room temperature. The technically marketed catalyst is called Hopcalite. It is very active in a highly disordered, often X-ray-amorphous state, but it has generally been observed to lose activity at temperatures above *ca.* 600 °C where crystallization of the spinel  $\text{CuMn}_2\text{O}_4$  occurs. The low temperature oxidation of CO has received renewed attention since Haruta *et al.* demonstrated that supported Au catalysts could be active at subambient temperatures.<sup>9,10</sup>

The high activity of the hopcalite catalyst is believed to be due to the resonance system  $\text{Cu}^{2+} + \text{Mn}^{3+} \rightleftharpoons \text{Cu}^{1+} + \text{Mn}^{4+}$  and the unique adsorption properties of carbon monoxide on  $\text{Cu}^{2+}/\text{Mn}^{4+}$  as well as of oxygen on  $\text{Cu}^{1+}/\text{Mn}^{3+}$ .<sup>11–13</sup> The purpose of the resonance system seems to be the regeneration of the catalyst in an active state after chemisorption of CO with respect to  $\text{O}_2$  and formation of  $\text{CO}_2$ . A typical synthesis method for the hopcalite systems is the coprecipitation of metal nitrates in aqueous solutions with  $\text{Na}_2\text{CO}_3$ . Hereby the “aging time” plays an important role on the activity of the catalyst. Furthermore, a multiphase system is generated.<sup>14</sup>

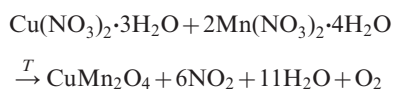
The complexity of the hopcalite systems (multiphase solids, electronic and structural promoters, *etc.*) makes it difficult to achieve information on the active sites of the catalyst, the mechanism of catalytic oxidation and the mechanisms of deactivation.

In this sense, and as a starting point in advanced metal oxide catalyst synthesis, it is advantageous to fabricate catalyst powders that contain – if possible – only the desired product phase.

The aim of this particular study was to generate pure and finely dispersed spinel-type metal oxides like  $\text{CuMn}_2\text{O}_4$ ,  $\text{LiMn}_2\text{O}_4$  and  $\text{CuCo}_2\text{O}_4$  by an aerosol decomposition procedure. A special contribution was made to the aerosol synthesis of  $\text{CuMn}_2\text{O}_4$  by introducing a fuel additive. Furthermore, a multitechnique characterization was applied for a conclusive characterization of the structural, thermochemical, morphological and catalytic properties of the solids generated by the ultrasonic thermal decomposition process.

## Experimental

A detailed description of the apparatus and synthesis conditions are published elsewhere.<sup>15</sup> The synthesis of the mixed metal oxide powders consists of three steps: atomisation of the metal nitrate solution; transport to the furnace system; and the controlled thermal decomposition of the aerosol. A typical equation for the overall reaction, *i.e.* the decomposition of the metal nitrates to the  $\text{CuMn}_2\text{O}_4$  spinel, can be formulated as follows:



Aqueous solutions of the metal nitrates were prepared by taking the appropriate molar ratio and a total metal ion concentration of 0.18 M. Solutions were atomised at 2 MHz, which yields aerosol particles with an average diameter of *ca.* 2  $\mu\text{m}$ . The generated aerosol is transported in  $\text{N}_2$  (flow rate 2.5 l  $\text{min}^{-1}$ ) into the furnace system, where preheating and the decomposition to the final product takes place. The decomposition temperature depends on the metal oxide system and lies between 450 and 950 °C. The herein investigated spinel systems  $\text{CuMn}_2\text{O}_4$ ,  $\text{LiMn}_2\text{O}_4$ ,  $\text{NiMn}_2\text{O}_4$  and  $\text{CuCo}_2\text{O}_4$  were all synthesized at a decomposition temperature of 650 °C. This relatively high temperature should facilitate the synthesis of sufficiently crystalline spinels. The cooled particles were collected on a fine pore quartz filter kept at 150 °C.

In order to achieve more direct influence over the textural and structural properties of the solids from the aerosol process, a modified synthesis procedure was developed. This was attained by introducing a fuel additive – glucose,  $\text{C}_6\text{H}_{12}\text{O}_6$  – into the starting metal nitrate solution. Real microreactors are designed, operating in the form of the individual precursor droplets, *i.e.* aerosol particles. Thus, each droplet of the aerosol is decomposed separately with changed thermal decomposition conditions. The synthesis of the metal oxides was performed with a 0.18 M metal nitrate solution with 0.03 or 0.06 mol glucose. The formed aerosol was transported in synthetic air (flow rate = 2.5 l  $\text{min}^{-1}$ ) to the furnace system ( $T_{\text{max}} = 650$  °C) where decomposition takes place.

$\text{CuMn}_2\text{O}_4$  was also synthesized by a common solid state synthesis in order to generate a standard product which can be compared with the one obtained by the aerosol process. The choice of the procedure was analogous to the one of Beley and coworkers, starting from  $\text{CuO}$  and  $\text{Mn}_2\text{O}_3$ .<sup>16</sup>

The obtained powders were investigated by means of atomic absorption spectroscopy (AAS), X-ray diffraction (XRD), thermoanalysis (TA), “pulsed-TA”, scanning electron microscopy (SEM), high resolution transmission electron microscopy (HRTEM), X-ray photoelectron spectroscopy (XPS) and  $\text{N}_2$ -physisorption.

The XPS spectra were all obtained using  $\text{MgK}\alpha$  radiation. Binding energies were calibrated with the  $\text{C1s}$  signal. The deconvolutions were performed with a Shirley-background and

approximated with Gaussian curves. Thermal surface gas treatments in He and surface reactions with CO and  $\text{O}_2$  were performed in a preparation chamber directly attached to the XPS spectrometer.

Catalytic tests were performed in a continuous flow fixed-bed micro-reactor with 200 mg of catalyst and a gas mixture of 3% CO and 3%  $\text{O}_2$  in He with a total flow rate of 30 ml  $\text{min}^{-1}$ . Catalyst temperature was kept at 325 K. In- and out-coming gas mixtures were analysed by on line gas chromatography. No previous drying of the gas mixtures (CO,  $\text{O}_2$ , He) was performed.

## Results and discussion

### Structural investigations and thermochemical behaviour of $\text{CuMn}_2\text{O}_4$

The spray pyrolysed  $\text{CuMn}_2\text{O}_4$  powders were analysed by AAS and gave an atomic ratio Mn : Cu = 1.75, which corresponds to the chemical formula  $\text{Cu}_{1.1}\text{Mn}_{1.9}\text{O}_4$ .

XRD patterns correspond to a cubic structure with a unit cell axis of 8.293 Å. Selected area electron diffraction gave no evidence of secondary phases. In samples synthesized at temperatures above 750 °C a second phase, *i.e.*  $\alpha\text{-Mn}_2\text{O}_3$ , is detected in low concentrations apart from the main product, *i.e.* the spinel.

The XRD patterns of all products prepared by the mentioned aerosol method showed significantly broadened reflections as compared to those resulting from either coprecipitations or high temperature synthesis of the same material. In all cases studied, the width of the broadened reflection could be diminished upon calcination at 400 °C without the appearance of new phases. For  $\text{CuMn}_2\text{O}_4$  an inert atmosphere was necessary.

Compared with  $\text{Cu}_{1.1}\text{Mn}_{1.9}\text{O}_4$  synthesized by solid–solid–reaction the unit cell axis of the “aerosol spinel” is 0.05 Å smaller, which corresponds to a cell reduction of 3%.<sup>17,18</sup> Reasons for this difference must be attributed to a new cationic configuration in the spinel lattice and the existence of cationic defects. The structural properties of  $\text{CuMn}_2\text{O}_4$  are known to depend crucially upon the synthesis conditions. Depending on the choice of the precursor, Beley *et al.* found tetragonal or cubic  $\text{CuMn}_2\text{O}_4$ .<sup>16</sup> Furthermore, the use of low temperature synthesis procedures allows the formation of cationic defects. A WAXS study of Laberty and coworkers on  $\text{NiMn}_2\text{O}_4$  (prepared from mixed manganese–nickel oxalate at 900 °C in air) indicates a high cationic defect concentration on tetrahedral sites.<sup>19</sup> The following formula can be written:  $\text{Ni(III)}_{0.35}\square_{0.65}\text{Ni(II)}_{0.27}\text{Ni(III)}_{0.16}\text{Mn(IV)}_{1.57}\text{O}_4$  ( $\square$  = tetrahedral cation vacancy). Similar effects are supposed to be the reason for the shortened unit cell axis for  $\text{CuMn}_2\text{O}_4$ , influenced also by the variety of different valencies of copper and manganese.

Investigations by means of XPS were performed in order to elucidate the surface composition of the studied metal oxides, but also in order to acquire detailed information on the chemical state of the cations and anions. Particularly, the valence states and the chemical environment are achievable. The  $\text{Cu2p}$  signal for complex spinel-type oxides indicates the existence of Cu(I) at 930.6 eV in a tetrahedral position and two species of Cu(II) at 932.2 and 934.0 eV, probably octahedrally and tetrahedrally coordinated (Fig. 1a, Table 1). Cu(I) in the octahedral position is improbable as its binding energy in spinel is found at values lower than 930 eV. The kinetic energy of the Auger  $\text{CuL}_{\text{VV}}$  region, *i.e.* the Auger parameter, makes a distinction of metallic and oxidized surface species possible. So, no metallic copper is found. The value of the  $\text{CuL}_{\text{VV}}$  signal is in agreement with studies of Jernigan and Somorjai who found kinetic energies at 918.5 eV for  $\text{Cu}^0$ , 916.5 eV for  $\text{Cu}_2\text{O}$  and 917.6 eV for  $\text{CuO}$ .<sup>20</sup>

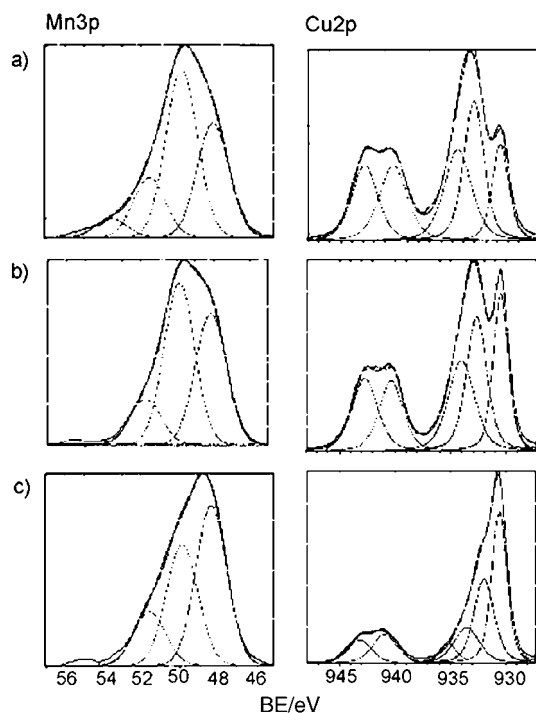


**Fig. 1** (a) Cu<sub>2p<sub>3/2</sub></sub> and Mn<sub>3p</sub> XPS spectra of as-pyrolysed Cu<sub>1.1</sub>Mn<sub>1.9</sub>O<sub>4</sub>; (b) heated for 1 h at 400 °C in N<sub>2</sub>; (c) heated for 1 h at 600 °C in N<sub>2</sub>.

The deconvolution of the Mn<sub>3p</sub> signal provides the manganese valencies. According to the XPS studies of Braber *et al.*,<sup>22</sup> Töpfer *et al.*,<sup>23</sup> and Allen *et al.*,<sup>24</sup> on several manganese-containing spinels, the Mn<sub>3p</sub> signal is useful to distinguish between the potential valencies Mn(II), Mn(III) and Mn(IV) (Fig. 1a). The deconvolution of the Mn<sub>3p</sub> signal shows a predominant existence of Mn(III) cations over Mn(II) and Mn(IV). This implies an overall predominance of Cu(II) and Mn(III) over Cu(I), Mn(II) and Mn(IV), respectively, lowering the cubic unit cell axis effected by smaller cation sizes. Obviously, the aerosol process offers a promising route to produce complex metal oxides with changed cationic distribution in the oxide matrix, especially for CuMn<sub>2</sub>O<sub>4</sub>.

Furthermore, the redox system  $\text{Cu}^{2+} + \text{Mn}^{3+} \rightleftharpoons \text{Cu}^{1+} + \text{Mn}^{4+}$  postulated in the hopcalite catalyst<sup>11,13</sup> is still found in the aerosol spinel, which is one of the main necessities for a successful catalytic performance. These results are in good agreement with the XPS studies of Lenglet *et al.* on copper-manganese-spinels, who found a partially inverted spinel.<sup>24</sup> Differences between a spinel from the aerosol method and that obtained *via* a common solid state synthesis are found in the concentration of the cations: the Cu(I) and Mn(IV) concentrations in the aerosol spinel are particularly low. Note the smaller intensity of the shake-up-satellites of the Cu<sub>2p</sub> region at 942 and 962 eV (Fig. 2). Reasons for this are the low temperature for the decomposition of the aqueous metal nitrate solution and the small residence time of the particles in the hot reaction zone of the furnace, so that the divalent copper cations cannot be reduced to the monovalent state.

**Table 1** XPS binding energies of Cu<sub>1.1</sub>Mn<sub>1.9</sub>O<sub>4</sub> for selected signals

Temperature of heating/°C	Cu <sub>2p<sub>3/2</sub></sub> (deconvolution)/eV			Mn <sub>3p</sub> /eV	CuL <sub>3VV</sub> <sup>a</sup> /eV
	Cu(I)	Cu(II) <sub>oct</sub>	Cu(II) <sub>tet</sub>		
As-pyrolysed	930.7(14)	933.0(45)	934.9(41)	49.8	917.9
400	930.5(24)	932.8(45)	934.5(30)	49.8	916.6
600	930.6(37)	932.0(39)	933.5(24)	48.8	916.7

<sup>a</sup>Kinetic energy (eV).

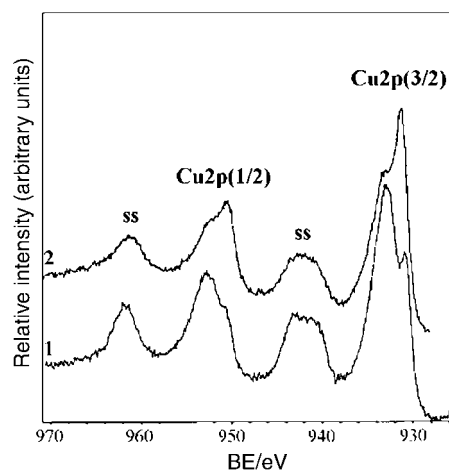


**Fig. 2** Cu<sub>2p</sub> region of CuMn<sub>2</sub>O<sub>4</sub> generated by the ultrasonic aerosol decomposition process (1) and, as a comparison, by a common solid state procedure (2).

The structural stability of the generated spinel shows different thermochemical behaviour in air or nitrogen. Whereas in air a marked tendency of phase segregation already at temperatures around 350 °C into Mn<sub>2</sub>O<sub>3</sub> and CuO is observed, the spinel is stable in nitrogen up to 600 °C. At temperatures higher than 600 °C a phase segregation under loss of oxygen and the formation of a tetragonal spinel with some parasitic phases is observed. The latest results on CuMn<sub>2</sub>O<sub>4</sub> from solid state synthesis indicate that the Cu(I)<sub>tet</sub> and Mn(IV)<sub>oct</sub> are the most stable configurations in the bulk.<sup>25</sup> Therefore, it is not surprising that the aerosol spinel with a major component of Cu(II) and Mn(III) is not stable at higher temperatures and segregates into the binary components. Furthermore, a loss of the cationic defect structure must be considered.

Heating the spray pyrolysed spinel up to 300 and 600 °C for 1 h in nitrogen, the unit cell axis of the simple cubic structure increases to  $a = 8.307$  and  $8.322$  Å, respectively. XPS results (Table 1) of the deconvoluted Cu<sub>2p<sub>3/2</sub></sub> and Mn<sub>3p</sub> signals indicate a change of the cationic- and valency-order.

While the as-pyrolysed spinel contains a very low content of Cu(I) in the tetrahedral coordination, the heated spinel increases its Cu(I) content by reducing the Cu(II) concentration (Fig. 1b and 1c). The binding energies of Cu<sub>2p<sub>3/2</sub></sub> for Cu(II) shift to lower values. The reason for this shift is the loss of water and hydroxide species while heating. Cu(OH)<sub>2</sub>, compared with other copper compounds with a divalent state, shows very high Cu<sub>2p</sub> binding energies.<sup>26</sup> The formation of metallic copper on the surface during heating cannot be confirmed as the Auger CuL<sub>2V</sub> kinetic energy points to mono- and di-valent copper cations.

The manganese cations also undergo a change, but in a less dominant manner. Particularly, the concentration of the trivalent species increases, whereas the concentrations of di- and four-valent states decrease but still exist. With increasing temperature an assimilation of the signals towards cationic distribution in CuMn<sub>2</sub>O<sub>4</sub> synthesized by a common solid state reaction takes place.

As will be shown later, the composition of the cations plays an important role for the activity of this spinel in the catalytic CO oxidation.

### Characterization of $\text{Cu}_x\text{Li}_{1-x}\text{Mn}_2\text{O}_4$ ( $0 < x < 1$ ), $\text{NiMn}_2\text{O}_4$ and $\text{CuCo}_2\text{O}_4$

The phase analysis of the spinels  $\text{Cu}_x\text{Li}_{1-x}\text{Mn}_2\text{O}_4$  ( $0 < x < 1$ ) and  $\text{CuCo}_2\text{O}_4$  by XRD confirm single phase products. Only for  $\text{NiMn}_2\text{O}_4$  is a small amount of  $\text{Mn}_2\text{O}_3$  observed apart from that of the spinel. Lattice parameters of the as-pyrolysed pure compounds are listed in Table 2.

The unit cell axis of  $\text{LiMn}_2\text{O}_4$  of the as-pyrolysed powder approximates the value in the literature for heating it for 1 h at  $400^\circ\text{C}$  in He.

$\text{CuCo}_2\text{O}_4$  cannot be obtained by conventional solid state reactions, but by low temperature synthesis methods. Petrov *et al.* describe the preparation of  $\text{Cu}_{0.92}\text{Co}_{2.08}\text{O}_4$  by the decomposition of metal nitrates at  $350^\circ\text{C}$ .<sup>27</sup> The spray-pyrolytic route is also a possibility to generate the desired product.

### Morphological characterization

The powder particles exhibit a spherical morphology. The average diameter depends both on the concentration of the solution and the frequency of the ultrasonic generator. Mean particle diameters are around  $0.7\ \mu\text{m}$  for a  $0.18\ \text{M}$  metal nitrate solution (Fig. 3) and  $0.3\ \mu\text{m}$  for a  $0.018\ \text{M}$  solution. The particle size distribution, determined by evaluating SEM micrographs, is in the range  $0.2\text{--}1\ \mu\text{m}$ . The form of the distribution isn't a pure Gaussian one because few droplets of the aerosol collide and/or agglomerate and thus form larger particles.

The particles consist of hollow spheres, which can be explained by the specific decomposition process of the aerosol droplets.<sup>28–30</sup>

The microstructure of a  $\text{CuMn}_2\text{O}_4$  spinel is shown in Fig. 4. The spheres consist of agglomerates composed of nanocrystallites of  $\text{CuMn}_2\text{O}_4$ . The diameter of the crystallites of an as-pyrolysed spinel averages  $1\text{--}2\ \text{nm}$ . The shape of the crystallites makes the occurrence of thermodynamically unrelaxed crystallographic orientations possible, so that very reactive sites towards CO and  $\text{O}_2$  are formed. HRTEM micrographs of  $\text{ZnFe}_2\text{O}_4$  made with the usual aerosol synthesis parameters but a higher decomposition temperature ( $950^\circ\text{C}$ ) show similar results with the difference of larger crystallite sizes, but still in a nanocrystalline form. As a consequence, these  $\text{ZnFe}_2\text{O}_4$  particles have a higher density.

### Surface area, porosity, catalytic tests and reactivity of the surface towards CO and $\text{O}_2$

Although many aerosol synthesis studies have described the preparation of materials that are known catalysts, few studies have actually examined their catalytic performance. Examples are found in studies of Hu and coworkers<sup>31</sup> who synthesized methanol synthesis catalysts, and in studies of Moser and coworkers<sup>5,6,32,33</sup> who synthesized perovskite-, spinel- and alkali-modified zinc oxide-catalysts. In many cases a better catalytic performance was achieved in comparison with conventionally synthesized catalysts.

**Table 2** Lattice parameters of different aerosol spinels

Phase	Lattice parameter/Å	Literature/Å
$\text{Li}_{0.2}\text{Cu}_{0.8}\text{Mn}_2\text{O}_4$	8.268	—
$\text{Li}_{0.5}\text{Cu}_{0.5}\text{Mn}_2\text{O}_4$	8.240	—
$\text{LiMn}_2\text{O}_4$	8.226	8.2476 <sup>a</sup>
$\text{CuCo}_2\text{O}_4$	8.111	8.105 [ref. 27]

<sup>a</sup>PDF-card 35-782.

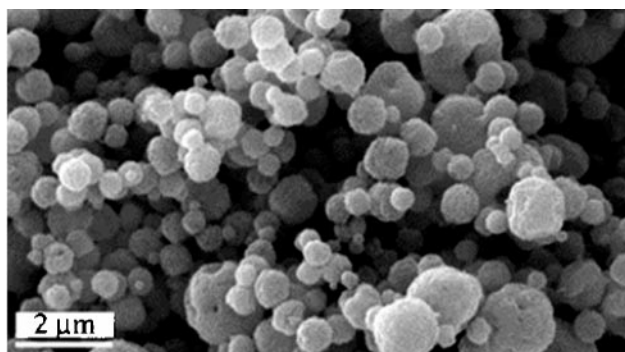


**Fig. 3** SEM of  $\text{Cu}_{1.1}\text{Mn}_{1.9}\text{O}_4$  from a  $0.18\ \text{M}$  nitrate solution ( $T_{\text{decomposition}} = 650^\circ\text{C}$ ).

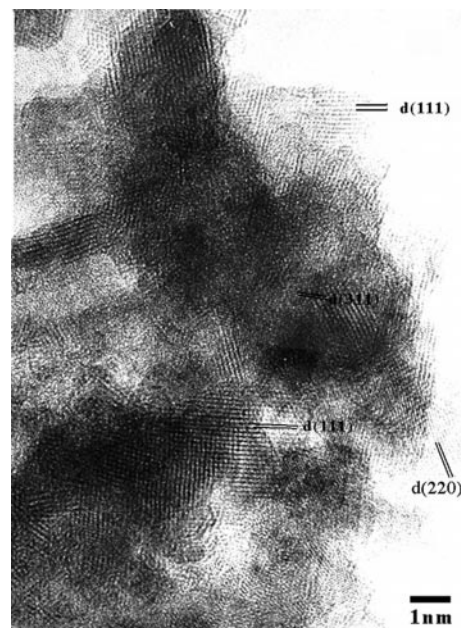


**Fig. 4** HRTEM of  $\text{CuMn}_2\text{O}_4$  from a  $0.18\ \text{M}$  metal nitrate solution ( $T_{\text{decomposition}} = 450^\circ\text{C}$ ).

The catalysts were subjected to a heating process for 1 h in He at various temperatures in order to clarify its influence on the CO conversion rate. As-pyrolysed spinels were inactive, whereas catalysts activated at moderate temperatures showed activity towards CO oxidation. Best results with respect to the highest conversion rates are obtained with an activation temperature of  $400^\circ\text{C}$ . Consequently all catalysts were subjected to this activation procedure. A reason for the necessity of thermal activation procedures is the coverage of the surface by water and hydroxide species, *i.e.* the metal centers of the catalyst must be activated first. This depends upon the choice of the solvent, *i.e.* water, in the aerosol synthesis procedure.

The surface area of three different manganese spinels (activated at  $400^\circ\text{C}$  in He for 1 h) lies between  $18$  and  $112\ \text{m}^2\ \text{g}^{-1}$ . These spinels –  $\text{CuMn}_2\text{O}_4$ ,  $\text{LiMn}_2\text{O}_4$  and  $\text{NiMn}_2\text{O}_4$  – all show a mesoporous behaviour according to the IUPAC nomenclature<sup>34</sup> with maxima of the pore size distribution of  $18.5$ ,  $50.5$  and  $5.5\ \text{nm}$ , respectively (Fig. 5).

Moser and coworkers<sup>32</sup> studied the influence of the decomposition temperature as well as the molarity of the solution in their aerosol process on the surface area. For iron oxide from nitrate solutions the surface area increased from *ca.*  $20$  to *ca.*  $88\ \text{m}^2\ \text{g}^{-1}$  with an increase in the decomposition

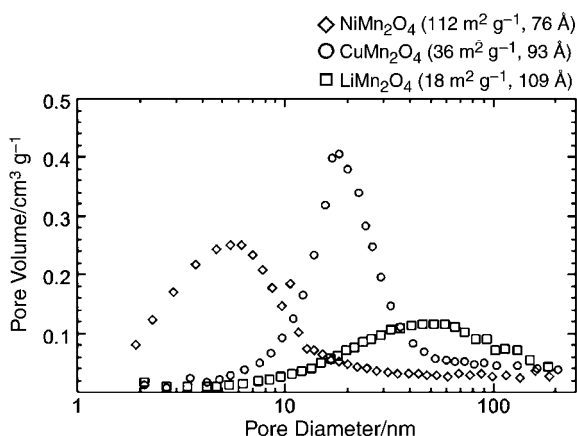


Fig. 5 Pore size distribution of  $\text{CuMn}_2\text{O}_4$ ,  $\text{LiMn}_2\text{O}_4$  and  $\text{NiMn}_2\text{O}_4$  (activated at  $400^\circ\text{C}$  in He for 1 h).

temperature from  $680$  to  $980^\circ\text{C}$ . Our values for activated  $\text{CuMn}_2\text{O}_4$  and  $\text{LiMn}_2\text{O}_4$  lie approximately in this range.

Conversion rates for the spinels  $\text{CuMn}_2\text{O}_4$ ,  $\text{LiMn}_2\text{O}_4$ ,  $\text{NiMn}_2\text{O}_4$  and  $\text{CuCo}_2\text{O}_4$  are shown in Fig. 6. Highest conversion rates are obtained for  $\text{CuMn}_2\text{O}_4$  with turnover rates of 100% during the first 120 min and a decrease in activity after 360 min to 75%.  $\text{NiMn}_2\text{O}_4$  and  $\text{CuCo}_2\text{O}_4$  also show high conversion rates but deactivate faster, whereas  $\text{LiMn}_2\text{O}_4$  is inactive. This behaviour points to the strong influence of the copper cations on the chemisorption processes of CO and  $\text{O}_2$  onto the catalyst.

It is possible to establish mixed valence states in the sense of a redox system for  $\text{NiMn}_2\text{O}_4$  and  $\text{CuCo}_2\text{O}_4$ . At ambient conditions the stable redox pairs  $\text{Ni}^{2+}/\text{Ni}^{3+}$  and  $\text{Co}^{2+}/\text{Co}^{3+}$  besides  $\text{Mn}^{3+}/\text{Mn}^{4+}$  are postulated as contributing to a high activity in the catalytic oxidation. For  $\text{LiMn}_2\text{O}_4$  only the manganese redox couple is existent. It effects no enhancement of the CO oxidation, although the manganese cations are coordinated in edge-sharing octahedra. The lithium cations are coordinated tetrahedrally and share only corners with neighbouring octahedra.

The reactivity of the surface of an aerosol spinel was tested with a thermally activated  $\text{CuMn}_2\text{O}_4$  catalyst towards CO–He-, CO– $\text{O}_2$ -,  $\text{O}_2$ –He-mixtures and  $\text{CO}_2$ . The XPS spectra of the spinel treated with CO– $\text{O}_2$  mixtures at RT over 1 h (Fig. 7) give no evidence of a chemical change of the cations on the surface. Only a higher intensity of the C1s signal due to adsorbed CO is observed. Treatment with CO at RT shows a reduction of both copper and manganese cations which points to a strong interaction of the CO molecules with the surface. Similar measurements on supported  $\text{CuO}/\text{NiO}/\gamma\text{-Al}_2\text{O}_3$  catalysts showed a remarkable effect with only 120 Torr of CO above  $100^\circ\text{C}$ . Full reduction of the copper cations was completed at  $550^\circ\text{C}$ .<sup>35</sup> “Pulsed TA” measurements with CO (1 ml per pulse) confirm these results, as after each pulse a weight loss and the production of  $\text{CO}_2$  is observed (Fig. 8). By increasing the number of the CO pulses the weight loss becomes smaller as the

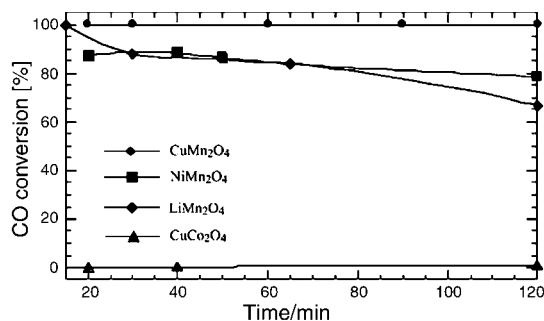


Fig. 6 CO conversion rates on different spinel-type oxides (for synthesis conditions, see text) activated at various temperatures.

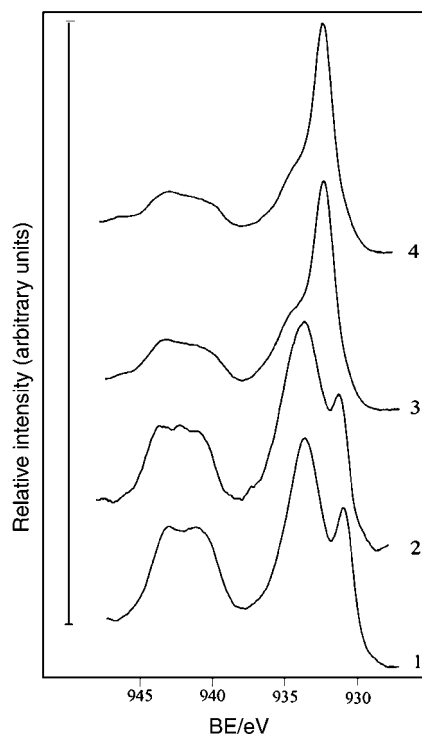


Fig. 7  $\text{Cu}2p_{3/2}$  region of  $\text{CuMn}_2\text{O}_4$  after the following gas treatments (total gas flow  $30\text{ ml min}^{-1}$ ): (1) activated at  $400^\circ\text{C}$  in He for 1 h; (2) 3.3% CO and 3.3%  $\text{O}_2$  in He at room temperature; (3) 3.3% CO in He at room temperature; (4) 3.3%  $\text{O}_2$  in He at  $150^\circ\text{C}$ .

active oxygen is consumed. The observed baseline shift of the TG curve can be explained by the presence of residual oxygen in the TG apparatus.

Reoxidation of the reduced surface with oxygen is not observed at room temperature by XPS, but at temperatures higher than  $150^\circ\text{C}$  a partial shift of the binding energies of both the  $\text{Cu}2p$  and  $\text{Mn}3p$  signals towards higher oxidation states of the cations is observed (Table 3).

#### The influence of glucose on the properties of $\text{CuMn}_2\text{O}_4$ formed in the aerosol, i.e. “droplet microreactors”

The introduction of glucose in the starting solution of the aerosol process was carried out for two reasons. First, the

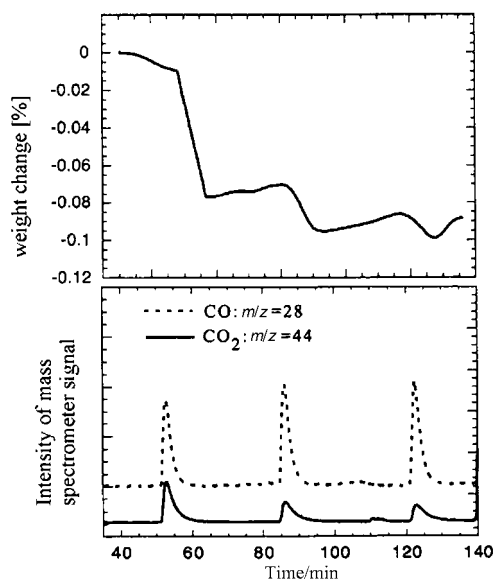


Fig. 8 “Pulsed thermoanalytical” measurement of  $\text{CuMn}_2\text{O}_4$  with CO (1 ml each pulse) at  $50^\circ\text{C}$ .

**Table 3** Binding energies of CuMn<sub>2</sub>O<sub>4</sub> after the following gas treatments: (total gas flow 30 ml min<sup>-1</sup>): (1) activated at 400 °C in He for 1 h; (2) 3.3% CO and 3.3% O<sub>2</sub> in He at room temperature; (3) 3.3% CO in He at room temperature; (4) 3.3% O<sub>2</sub> in He at 150 °C

No.	Cu2p <sup>a</sup>			Cu3p	Cu3s	Mn2p	Mn3p	O1s	CuLVV Kinetic energy/eV
	Binding energy/eV								
1	930.8	932.8	934.5	76.5	123.0	642.0	49.9	529.8	917.9
2	930.5	932.7	934.4	76.3	123.1	641.9	49.4	530.0	917.7
3	931.5	932.5	934.0	75.1	—	641.2	48.2	530.0	916.7
4	—	—	—	75.5	123.1	641.7	48.4	529.8	917.2

<sup>a</sup>Binding energies from the deconvolution of Cu2p<sub>3/2</sub> signals.

energy required to obtain the metal oxides should be introduced in chemical form to the spherical aerosol particles. So the powders are generated by utilizing both external heating and internal chemical energy released during combustion. Second, the change of the textural and structural properties of the spinels should be studied. Above all, the influence of a new surface cationic configuration on the already mentioned redox system  $\text{Cu}^{2+} + \text{Mn}^{3+} \rightleftharpoons \text{Cu}^{1+} + \text{Mn}^{4+}$  and the turnover rate of the catalytic CO oxidation should be studied. The synthesis parameters and some of the properties of CuMn<sub>2</sub>O<sub>4</sub> (activated at 400 °C in He) are listed in Table 4. TG/DTA measurements on the decomposition of the metal nitrates, glucose and mixtures of the two components indicate a striking effect of glucose on the enthalpy changes during reaction to the metal oxide (Fig. 9). While the metal nitrate decomposition is endothermic, the use of glucose alters the overall reaction to an exothermic one, on starting the decomposition already at 150 °C.

Furthermore, the decomposition of glucose generates reducing product gases like CH<sub>4</sub>, H<sub>2</sub>, etc. which might have an influence on the surface and bulk properties of the solids.

The reaction between the strongly oxidizing anion (NO<sub>3</sub><sup>-</sup>) and the product gases is extremely exothermic, which causes heating of the order of several hundred degrees and may also be explosive. But as in the aerosol process a controlled introduction of only small quantities of the precursor mixtures is possible, no problems arise with this. The measured exo- and endo-thermic reactions are influenced by the heating rate. In the form of a simulation, DTA measurements are a helpful tool for the prediction of the transformed energies.

The introduction of glucose has a great influence on the microstructure and the valency distribution of the cations Cu and Mn. The as-pyrolysed solid is received in an amorphous state, no reflections are observed in the XRD pattern. The common thermal activation of these solids at 400 °C generates a crystalline spinel powder, assuming a very homogenous distribution of the cations in the as-pyrolysed product. The distribution shifts towards Cu(II) and Mn(II). Cu(II), Mn(III) and Mn(IV) are found in a lower concentration compared to the spinels synthesized by the conventional method with metal nitrate only. Fig. 10 shows a comparison of the Cu2p and Mn3p signals of the two samples of CuMn<sub>2</sub>O<sub>4</sub>. Note the striking decrease of the turnover rates between the two catalysts. The redox system  $\text{Cu}^{2+} + \text{Mn}^{3+} \rightleftharpoons \text{Cu}^{1+} + \text{Mn}^{4+}$

**Table 4** Synthesis conditions and selected properties of CuMn<sub>2</sub>O<sub>4</sub>

	With glucose	Without glucose
Glucose concentration/M	0.06	0.06
Metal nitrate concentration/M	0.18	0.18
Structure	Spinel <sup>a</sup>	Spinel <sup>a</sup>
Surface area/m <sup>2</sup> g <sup>-1</sup>	44.6	39.6
Porosity	Mesoporous	Mesoporous
Cu(I)/Cu(II)	47/53 <sup>b</sup>	24/76 <sup>b</sup>
CO turnover rate (%)	4.6	100

<sup>a</sup>Activated at 400 °C in He. <sup>b</sup>From deconvolution of the XPS Cu2p signal.

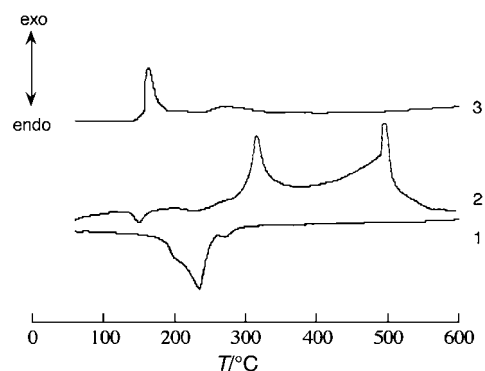


**Fig. 9** Differential thermal analysis scans of (heating rate 20 C min<sup>-1</sup>): (1) Cu(NO<sub>3</sub>)<sub>2</sub>·3H<sub>2</sub>O, Mn(NO<sub>3</sub>)<sub>2</sub>·4H<sub>2</sub>O (mixture with stoichiometry 1:2), dried at 150 °C; (2) glucose; (3) Cu(NO<sub>3</sub>)<sub>2</sub>·3H<sub>2</sub>O/Mn(NO<sub>3</sub>)<sub>2</sub>·4H<sub>2</sub>O/glucose mixture (stoichiometry 1:2:1), dried at 150 °C.

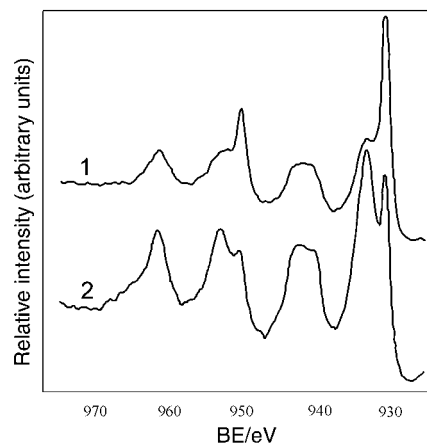


**Fig. 10** Comparison of the Cu2p region of CuMn<sub>2</sub>O<sub>4</sub> synthesized with (2) and without glucose (1).

seems to accomplish its role only in a narrow distribution of the surface concentration of the cation. High concentrations of Cu(II), Mn(III) and Mn(IV) besides a low concentration of Cu(I) increase the activity of the spinel catalyst markedly, whereas high concentrations of Cu(I) and Mn(II) results in a lower activity. Other known deactivation processes such as segregation of non-active species (e.g. potassium)<sup>11</sup> to the surface or high carbon content on the surface were not registered by XPS.

Hardly any effects from the use of glucose are found in the morphology of the aerosol powders. Spheres are still found, but few are fragmented to smaller particles (Fig. 11a and 11b).

## Conclusion

The described spray-pyrolytic process for the reproducible generation of nanocrystalline mixed metal oxides offers a promising route to catalytically active materials. The one-step

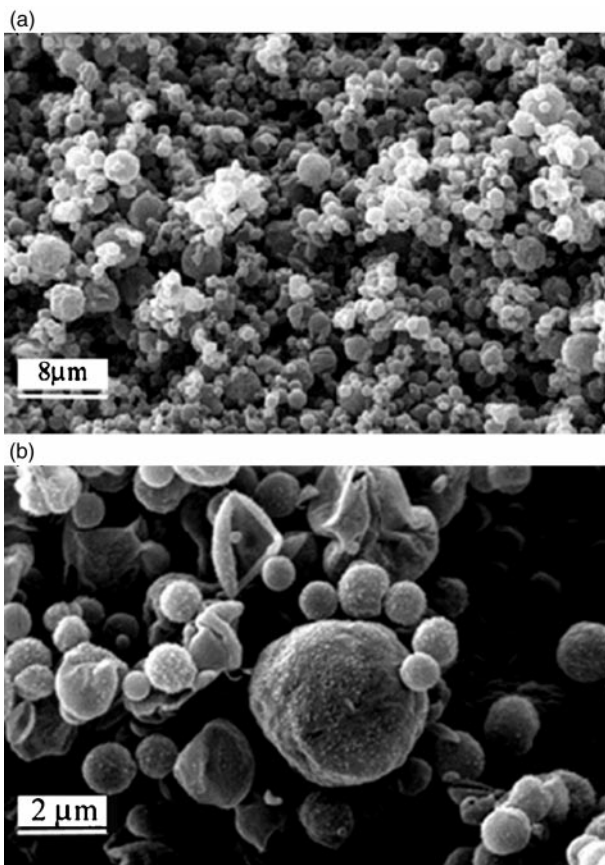


Fig. 11 (a and b) SEM images of  $\text{CuMn}_2\text{O}_4$  synthesized with glucose (0.03 M solution).

process starting from simple metal nitrate precursors produces finely dispersed and homogeneous powders with regular shape.  $\text{N}_2$ -physisorption measurements on several spinels show high surface areas and a mesoporous pore size distribution.

The cationic- and valency-order of  $\text{CuMn}_2\text{O}_4$  are changed in comparison with spinels synthesized by conventional solid state reactions. Reasons for this behaviour are the special reaction mechanism of our procedure, with short reaction time and moderate decomposition temperature, which prevents a relaxation of the cations to a thermodynamically more stable state.

The catalytic experiments gave evidence of the high activity of  $\text{CuMn}_2\text{O}_4$  towards CO, but also  $\text{NiMn}_2\text{O}_4$  and  $\text{CuCo}_2\text{O}_4$  showed high activity during the first 60 minutes. As it has been suspected, spinel formation in amorphous Cu–Mn catalysts can be a promoter of CO oxidation; this study supports this opinion indeed. The tests showed that turnover rates depend upon the activation temperature of the spinels.

The use of fuel additives in the starting solution of this particular synthesis procedure allows the generation of fine spinel powders with a unique combination of chemical properties. In general, only the cationic distribution on the surface is changed from a high  $\text{Cu(II)}$  content without introduction of glucose in the starting solution to an equilibrated distribution of  $\text{Cu(I)}/\text{Cu(II)}$  ratio with the use of glucose. The distribution of  $\text{Cu(I)}$  and  $\text{Cu(II)}$  has dramatic

consequences for the activity of the catalyst. A high  $\text{Cu(I)}$  concentration on the surface causes a decrease of the turnover rate of CO oxidation. This also implies that the resonance system is perturbed and can no longer influence the catalytic reaction.

## References

- 1 T. T. Kodas, *Adv. Mater.*, 1989, **101**, 814.
- 2 N. Tohge, S. Tamaki and K. Okuyama, *Jpn. J. Appl. Phys.*, 1995, **34**, L207.
- 3 N. Mizutani and T. Liu, *Ceram. Trans.*, 1990, **12**, 59.
- 4 A. R. Raju and C. N. R. Rao, *Appl. Phys. Lett.*, 1995, **66**(7), 896.
- 5 W. R. Moser, J. D. Lennhoff, J. E. Clossen, K. Fraska, J. W. Schoonover and J. R. Rozak, in *Advanced Catalysts and Nanostructured Materials*, W. R. Moser, ed., Academic Press, 1996, pp. 535–562.
- 6 W. R. Moser, in *Catalytic Selective Oxidation*, S. T. Oyama and J. W. Hightower, ed., ACS, Washington, 1993, ACS Symp. Ser. vol. 523, pp. 244–260.
- 7 T. Gonzalez-Carreño, *Mater. Lett.*, 1993, **18**, 151.
- 8 C. B. Martin, R. P. Kurosky, C. D. Maupin, C. Han, J. Javadpour and I. A. Aksay, *Ceram. Trans.*, 1990, **12**, 99.
- 9 M. Haruta, S. Tsubota, T. Kobayashi, H. Kageyama, M. J. Genet and B. Delmon, *J. Catal.*, 1993, **144**, 175.
- 10 M. Haruta, N. Yamada, T. Kobayashi and S. Iijima, *J. Catal.*, 1989, **115**, 301.
- 11 S. Veprek, D. L. Cocke, S. Kehl and H. R. Oswald, *J. Catal.*, 1986, **100**, 250.
- 12 G. Schwab, *Chem.-Ing.-Tech.*, 1972, **44**(16), 957.
- 13 D. L. Cocke and S. Veprek, *Solid State Commun.*, 1986, **57**, 745.
- 14 G. J. Hutchings, A. A. Mirzaei, R. W. Joyner, M. R. H. Siddiqui and S. H. Taylor, *Catal. Lett.*, 1996, **42**, 21.
- 15 P. Fortunato, A. Reller and H. R. Oswald, *Solid State Ionics*, 1997, **101–103**, 85.
- 16 M. Beley, L. Padel and J. C. Bernier, *Ann. Chim. (Paris)*, 1978, **3**, 429.
- 17 R. Buhl, *J. Phys. Chem. Solids*, 1969, **30**, 805.
- 18 R. Vandenberghe, G. G. Robbrecht and V. A. M. Brabers, *Mater. Res. Bull.*, 1973, **8**, 571.
- 19 C. Laberty, M. Verelst, P. Lecante, P. Alphonse, A. Mosset and A. Rousset, *J. Solid State Chem.*, 1997, **129**, 271.
- 20 G. Jernigan and G. A. Somorjai, *J. Catal.*, 1994, **147**, 567.
- 21 V. A. M. Brabers, F. M. V. Setten and P. S. A. Knapen, *J. Solid State Chem.*, 1983, **49**, 93.
- 22 J. Töpfer, A. Feltz, D. Gräf, B. Hackl, L. Raupach and P. Weissbrodt, *Phys. Status Solidi*, 1992, **134**, 405.
- 23 G. C. Allen, S. J. Harris, J. A. Jutson and J. M. Dyke, *Appl. Surf. Sci.*, 1989, **35**, 111.
- 24 M. Lenglet, A. D'Huysser, J. Kasperek, J. P. Bonnelle and J. Dürr, *Mater. Res. Bull.*, 1985, **20**, 745.
- 25 R. E. Vandenberghe, *Phys. Status Solidi*, 1987, **50**, K85.
- 26 D. Frost, A. Ishitani and C. A. McDowell, *Mol. Phys.*, 1972, **24**, 861.
- 27 K. Petrov, T. Karamaneva, S. Agelov and D. Mehandjiev, *Mater. Res. Bull.*, 1983, **18**, 637.
- 28 D. W. Sproson and G. L. Messing, *Adv. Ceram.*, 1987, **21**, 99.
- 29 S. C. Zhang and G. L. Messing, *Ceram. Trans.*, 1990, **12**, 49.
- 30 D. Majumdar, T. A. Shefelbine, T. T. Kodas and H. D. Glickman, *J. Mater. Res.*, 1996, **11**, 2864.
- 31 Y. H. Hu, H. Wan and K. R. Tsai, *J. Nat. Gas Chem.*, 1994, **3**, 280.
- 32 W. R. Moser, *Chem. Eng. Commun.*, 1989, **83**, 241.
- 33 W. R. Moser, *Catal. Today*, 1994, **21**, 157.
- 34 K. S. W. Sing, D. H. Everett, R. A. W. Haul, L. Moscou, R. A. Pierotti, J. Rouquérol and T. Siemie-niewka, *Pure Appl. Chem.*, 1985, **57**, 603.
- 35 N. Thiele, Inaugural Dissertation, Photolektronenspektroskopische Untersuchungen an Katalysatoroberflächen, Ludwigs-Maximilians-Universität München, 1979.